

# Pion electromagnetic formfactor in the instanton vacuum

Andree Blotz <sup>\*</sup> and Edward Shuryak <sup>†</sup>

*Department of Physics, State University of New York in Stony Brook,  
NY 11794-3800, USA*

(August 26, 2018)

SUNY-NTG-9-96)

## Abstract

We have calculated the 3-point correlation function for the electromagnetic interaction of the pion in an ensemble of instantons and anti-instantons, modelling the QCD vacuum. The results are well described by a pion pole and the pion formfactor is extracted, nicely following a standard monopole fit. The experimental data on the formfactor are well reproduced, provided an average instanton size is fixed at  $\bar{\rho} = 0.35 \pm 0.03$  fm, the same as found for a variety of other correlation functions and was found on the lattice.

---

<sup>\*</sup>email:andree.blotz@sunysb.edu

<sup>†</sup>email:edward.shuryak@sunysb.edu

## I. INTRODUCTION

Significant progress has been made during the last few years in understanding of the QCD vacuum and hadronic structure in terms of instantons. In a series of papers [1–3] it has been shown that a specific model, which assumes ensembles of instantons and anti-instantons in the QCD vacuum, can not only describe the gross features of the vacuum, such as spontaneous chiral symmetry breaking or topological susceptibilities<sup>1</sup>, but can also *quantitatively* describe a large number of mesonic and baryonic correlation functions, in agreement with phenomenology [5] and lattice calculations [6]. Furthermore, the parameters of the ensemble have been confirmed by lattice studies [7,8], and also the dominant role of instantons was directly demonstrated by removal of all other kinds of the gauge fields from the configurations by the so called *cooling* procedure [7].

In view of those developments, wider practical applications of the instanton-based models are justified. Since studies of 2-point correlators have produced hadronic masses and coupling constants in agreement with data, it is natural to perform more detailed studies and test whether those models can or cannot describe details of hadronic structure as well. Three point correlation functions can describe hadronic couplings to external fields, and for this aim they have been considered within the QCD sum rule approach (e.g. [9]), the light-cone formalism (e.g. [10,11] ), the generalized impulse approximation within non-perturbative Dyson-Schwinger equations [12] and of course on the lattice [13–15].

Only very recently the first (and the simplest) 3-point function related with the pion formfactor has been studied in the so called single-instanton approach by Forkel and Nielsen [16]. For  $Q^2 \sim 1 \text{ GeV}^2$  they have found good agreement with data.

---

<sup>1</sup>See e.g. [4] for a recent review of chiral symmetry breaking mechanism by instantons

Significant advantage of their approach over the previous QCD sum rule calculation is that the *pseudoscalar* (rather than the axial) currents are used in order to create pions. It makes a significant practical difference, because the pion is coupled to the former current with large constant  $\lambda_\pi$  and to the latter with the small coupling  $f_\pi$ .

Technically Forkel and Nielsen follow closely ref. [17] in which the 2-point pion correlator was discussed in the single-instanton approximation: in it the propagators are calculated using the zero-mode solution of the Dirac operator in the presence of one close instanton (or anti-instanton), whereas the effect of the remote instantons is taken into account in some mean field approximation. This is a good approximation, provided all relevant distances  $(x, y)$  are short compared to inter-instanton separation  $R \sim 1 \text{ fm} \gg (x, y) \sim 0.2 \text{ fm}$ . In practice, it is a very important limitation, since it does not allow to separate the pole term from the non-pole or “continuum” contributions unambiguously. Therefore Forkel and Nielsen had to extract the formfactor by a complicated fitting procedure, similar to what is done in the context of QCD sum rules. Also, they have performed a traditional Borel transform of the correlator, while in fact the whole analysis can better be made directly in (Euclidean) space-time representation, in which all relevant formulae are much simpler.

In the present paper we also study with better accuracy a variety of two point correlation functions, and check how the obtained masses of hadrons are correlated with hadronic formfactors. The electromagnetic form factor of the pion is of special interest, because the pion is the Goldstone boson of the spontaneously broken chiral symmetry and therefore the quark attraction in this channel is very large. Furthermore in the models used the pion is bound by instanton-induced forces, and in a way its formfactor is basically the instanton formfactor.

We are using the methods developed in [1] which allow to evaluate quark propagators in a multi-instanton background numerically, up to rather large distances.

Therefore, we are *not* restricted to small  $x, y \ll R$  and thus have no significant “background” from non-pion states. As a result, we can extract the pion formfactor with much better accuracy, and even study how it depends on various modifications of the underlying ensemble. Since the pion formfactor is also relatively accurately measured, those studies proved to provide a very rigid constrained on such microscopic parameters such as the mean instanton size.

We use two formulations of the statistical instanton-based models: the simplest Random Instanton Liquid Model (RILM) [18,1,2] and the much more developed Interacting Instanton Liquid Model (IILM) [19,20]. While the former one has simply the previously determined total instanton density and average size as input and assumes a random distribution in all collective coordinates, the latter one is a statistical model which predicts correlations between the instantons in the liquid. Some of those correlations are known to be qualitatively important: e.g. quark-induced interactions lead to a screening of the topological charge and correct the large distance behaviour of the correlators in channels, where the random model produces repulsion [21]. It is also important that in the IILM the instanton parameters were not fixed but determined selfconsistently, and after the instanton interaction is fixed the only parameter left is  $\Lambda_{QCD}$ . If its value is fixed from an average density of  $\bar{n} = 1 \text{ fm}^{-4}$ , an average instanton size which emerges is somewhat larger than the original  $\rho = 1/3 \text{ fm}$  [18] or recent lattice results [7,8].

The organization of the paper is as follows. In section II. we summarize the phenomenological knowledge of the 3 point correlation function for the pion. In section III. we show how to derive this correlator within the Instanton Liquid model and show also the various short distance approximations to the full simulation. Sect. IV discusses the numerical procedure and results for the RILM and sect. V for the IILM. In sect. VI we make some concluding remarks. The App. A. gives some formulas for the direct

instanton approach and App. B gives formulas for the continuum contribution of the 3 point function.

## II. ELECTROMAGNETIC PION FORM FACTOR - NOTATIONS AND PHENOMENOLOGY

The electromagnetic structure of the pion can be measured in the time-like region, the  $\rho$ -meson pole containing part of the formfactor or structure function and in the space-like part. In both cases the formfactor depend only on the four-momentum transfer of the pion which we denote by  $Q^2 = -q^2$ . (Below we always use space-like momenta,  $Q^2 > 0$ .) While the time-like region can be investigated in collider experiments such as  $e^+e^- \rightarrow \pi^+\pi^-$ , the space-like region is obtained from scattering of pions off atomic electrons (for small  $q^2$ ) or via the production of pions in  $e^-p \rightarrow e^-\pi^+n$  (for larger  $q^2$ ).

From the theoretical point of view the interaction of the hadrons with external currents like the electromagnetic one is most conveniently written in terms of three point correlation functions. The three points denote the creation and annihilation points of the hadrons as well as the location of their interaction with the external current  $j_\mu^Q(y)$ :

$$\Pi_\mu(\bar{p}, q) = \int d^4x \int d^4y e^{i\bar{p}x} e^{iqy} \langle 0 | \mathcal{T} j_5^{\pi^\dagger}(-x/2) j_\mu^Q(y) j_5^\pi(x/2) | 0 \rangle \quad (1)$$

where  $\bar{p} = (p + p')/2$  is the average of the momenta  $p, p'$  connected to the pseudoscalar currents. The charged pions are represented by the quark bilinears

$$j_5^{\pi^\pm}(x) = \begin{pmatrix} \bar{d}(x) i\gamma_5 u(x) \\ \bar{u}(x) i\gamma_5 d(x) \end{pmatrix} = \frac{1}{\sqrt{2}} \bar{q}(x) i\gamma_5 \tau^\pm q(x) := \bar{q}(x) \Gamma_\phi q(x) \quad (2)$$

and  $j_\mu^Q(y) = \bar{q}(x) Q \gamma_\mu q(x) = \sum_{i=u,d} e_i \bar{q}_i(y) \gamma_\mu q_i(y)$  is the electromagnetic current.

The 3-point function in the r.h.s. of eq. (1) is the quantity we will calculate below. Its transform, the l.h.s. of eq. (1), can be related to physical observables by a double dispersion relation [22]<sup>2</sup>

$$\Pi_\mu(\bar{p}, q) = \int_0^\infty ds_1 \int_0^\infty ds_2 \frac{\rho_\mu(s_1, s_2, Q^2 = -q^2)}{(s_1 - p^2)(s_2 - p'^2)} \quad (3)$$

over the spectral density  $\rho_\mu(s_1, s_2, Q^2 = -q^2) = \rho_1(s_1, s_2, Q^2)\bar{p}_\mu + \rho_2(s_1, s_2, Q^2)q_\mu$ . As explained below, the e.m. formfactor of the pion can be extracted from the former structure containing  $\bar{p}_\mu$  and  $\rho_1(s_1, s_2, Q^2)$ .

A Borel transformation in  $p$  and  $p'$  was used in earlier papers, with the purpose to eliminate the polynomial subtraction terms. Our philosophy is however different: we make an inverse Fourier transfer to coordinate representation instead, in which the propagators in the instanton background are naturally obtained. As shown in details in [5] for the 2-point functions, the coordinate space is as good as Borel representation for all our purposes.<sup>3</sup> The second reason for using the Borel transform in QCD sum rules, namely to suppress the larger mass resonances, is also not needed here, because in the coordinate-space correlator these states are automatically suppressed at distances we will work with.

The spectral density  $\rho_\mu(s_1, s_2, q^2)$  is proportional to the imaginary part of the polarization operator. We approximate it as the pion contribution given by

---

<sup>2</sup>The double integral is needed because one has to use a complete set of physical states both in the incoming and the outgoing channel. For a recent discussion on the dispersion relations cf. [23,24]. Although the eq. (3) is not well defined due to the divergent behaviour of the dispersion integral for large momenta  $s, s'$ , one can improve that by subtraction of polynomials functions of  $p^2, p'^2, Q^2$ .

<sup>3</sup> As we show in App. B., the coordinate space representation of eq. (3) is not only finite but reproduces also the correct short distant behaviour.

$$\rho_{pole}(s_1, s_2, q^2) = (2\pi)^3 \delta(s_1 - m_\pi^2) \delta(s_2 - m_\pi^2) \langle 0 | j_5(0) | \pi \rangle \langle \pi | j_\mu^Q | \pi \rangle \langle 0 | j_5(0) | \pi \rangle \quad (4)$$

Here the overlap matrix element

$$\langle 0 | j_5(x) | \pi(p) \rangle = \lambda_\pi (2\pi)^{-3/2} e^{ipx} \quad (5)$$

is given in terms of  $\lambda_\pi$ , which may be represented as [19]

$$\lambda_\pi = \frac{\bar{q}q}{\sqrt{2}f_\pi} = \frac{\sqrt{2}\bar{u}u}{f_\pi} \quad (6)$$

with  $f_\pi$  corresponding to the experimental  $f_\pi = 93$  MeV. The definition of the electromagnetic form factor  $F_\pi(q^2)$  eq. (4) is

$$\langle \pi(p) | j_\mu(0) | \pi(p') \rangle = e_\pi F_\pi(q^2) 2\bar{p}_\mu, \quad (7)$$

which is normalized by  $F_\pi(0) = 1$ . Then the eq. (4) can be written as

$$\Pi_\mu(\bar{p}, q) = \frac{\lambda_\pi^2 2e_\pi F_\pi(q^2)}{((\bar{p} - q/2)^2 + m_\pi^2)((\bar{p} + q/2)^2 + m_\pi^2)} \bar{p}_\mu + \Pi_{\mu,cont}(\bar{p}, q) \quad (8)$$

with free quark continuum  $\Pi_{\mu,cont}(\bar{p}, q)$  (cf. App. B), starting at some threshold value  $s_0$ .

The experimental measured form factor in the space like region has been shown to be well parametrized by a monopole form factor [25,26], resembling in some way the exchange of a  $\rho$  meson in *vector dominance* models. The parameter in this fit with  $m_V = 679 \pm 19$  MeV [25] is however below the  $\rho$  meson mass<sup>4</sup> The measurements are performed over the large range<sup>5</sup> of space-like  $Q^2 = 0.18 - 9.77$  GeV<sup>2</sup>. In coordinate

---

<sup>4</sup>There is also a precise measurement of the formfactor for smaller  $Q^2 < 0.30$  GeV<sup>2</sup> [26], which yields, also from a monopole fit,  $m_V = 736 \pm 9$  MeV and is still below the  $\rho$  mass.

<sup>5</sup>See also the CEBAF proposal [27] for a future high statistics measurement of the formfactor via electroproduction at  $Q^2 \simeq 0.5 - 5$  GeV<sup>2</sup>.

space this measures the region around 0.05–0.5 fm. The upper limit of which is clearly dominated by non-perturbative effects in the QCD vacuum, as will be shown, and in general cannot be described by the operator product expansion.

The fourier transform of eq. (8) is then conveniently calculated from

$$\begin{aligned} \Pi_{\mu,pole}(x, y) = & -i \int_0^\infty dq \int_0^1 d\alpha \frac{q^2}{32\pi^4} \frac{J_1(q |y - x(0.5 - \alpha)|)}{|y - x(0.5 - \alpha)|} \sqrt{m_\pi^2 + q^2\alpha(1 - \alpha)} \\ & K_1 \left( |x| \sqrt{m_\pi^2 + q^2\alpha(1 - \alpha)} \right) \frac{2\lambda_\pi^2 e_\pi}{1 + q^2/m_V^2} \frac{x_\mu}{|x|} \end{aligned} \quad (9)$$

where  $J_1, K_1$  are the normal and modified bessel functions. The rather cumbersome formula for the continuum is given in App. B. In eq. (9) we used already the monopole parametrization of the form factor [25], which was shown to be a good description in the space like region of the form factor.

### III. THE INSTANTON LIQUID

The 3-point function in question can be evaluated using the same quark propagators in the multi-instanton background fields as used for the 2-point functions in [19,20], and we will not repeat any details here. The generating functional of the IILM can be written as

$$\begin{aligned} Z[\eta, \bar{\eta}, s_\mu^a] = & \frac{1}{N_+!N_-!} \int \prod_i^{N_++N_-} d\Omega_i d(\rho_i) e^{-\int d^4x d^4y \bar{\eta}(x) [(\hat{D} + m_f - s_\mu^a \Gamma_\mu^a)(x, y)]^{-1} \eta(y)} \\ & e^{(-S_{int})} \prod_f^{N_f} \det \left( \hat{D} + m_f - s_\mu^a \Gamma_\mu^a \right) \end{aligned} \quad (10)$$

We will only shortly explain the meaning of the various expressions. The  $\hat{D}$  is the fermionic Dirac operator in the presence of instantons and anti-instantons. These instanton solutions are described by a set of collective coordinates  $\Omega_i$ , which are the color orientation  $U_i$ , the position  $z_i$  and the size  $\rho_i$  of the instanton. Therefore the original gauge measure  $\mathcal{D}A_\mu$  becomes essentially an integral over the collective coordinates  $d\Omega_i$ .



The  $d(\rho_i)$  in eq. (10) is the semiclassical instanton amplitude, which was originally calculated by 't Hooft: its two-loop version is used in [19].

The  $m_f$  are the explicit (chiral and vector) symmetry breaking current masses and  $S_{int}$  denotes the classical interaction of the instantons, which is as usual [19] approximated by a two-body interaction.

In the case of the electromagnetic formfactor one has  $\Gamma_\mu^Q = \gamma_\mu Q^a \tau^a$ , where  $Q$  is the electromagnetic charge matrix. The spin-isospin matrices  $\Gamma_\phi$ , ( $\phi = \pi, \delta$ ), in eq. (2) correspond to  $i\gamma_5 \tau^\pm / \sqrt{2}$  for the charged pions  $\pi^\pm$  and to  $\tau^\pm / \sqrt{2}$  for the isovector scalar  $\delta$ -meson. The reason to discuss also the  $\delta$  shortly will become clear in the following. From the generating functional eq. (10) a three point correlator for a mesonic state is obtained from

$$\Pi_\mu(x, y) = (\Gamma_\phi)_{ab}^{\alpha\beta} (\Gamma_\phi)_{cd}^{\gamma\delta} \frac{\delta}{\delta s_\mu^Q(y)} \frac{\delta^4 Z[\eta, \bar{\eta}, s_\mu^a]}{\delta \bar{\eta}_a^\alpha(-x/2) \delta \eta_b^\beta(-x/2) \delta \bar{\eta}_c^\gamma(x/2) \delta \eta_d^\delta(x/2)} \quad (11)$$

where latin indices correspond to spin indices and greek symbols to isospin indices. Since all currents of interests are color singlets, color indices are implicitly understood. In terms of the quark propagators the general form for the 3-point correlator, using isospin symmetry for the up and down quark propagator  $S_u = S_d$ , follows as

$$\begin{aligned} \Pi_\mu(x, y) = & (e_u - e_d) (\langle \text{tr} S(-x/2, y) \gamma_\mu S(y, x/2) \gamma_5 S(x/2, -x/2) \gamma_5 \rangle - \\ & \langle \text{tr} S(y, y) \gamma_\mu \text{tr} S(-x/2, x/2) \gamma_5 S(x/2, -x/2) \gamma_5 \rangle - \\ & \langle \text{tr} S(y, y) \gamma_\mu \text{tr} S(-x/2, -x/2) \gamma_5 \text{tr} S(x/2, x/2) \gamma_5 \rangle) \end{aligned} \quad (12)$$

Since the quark propagators in eq. (12) are evaluated in a given instanton anti-instanton background, averaging over different instanton ensembles is implicitly understood by the brackets in eq. (12). Here the first term on the RHS of eq. (12) is the so called connected contribution and the second and third are the disconnected diagrams. One should note of course that the quark propagators are the full propagators in the background of the multi instanton/anti-instanton configurations so that the expression

'disconnected' refers only to the 'quark lines'. One may note that the disconnected terms are in general obtained from the fermion determinant of the generating functional eq. (10) <sup>6</sup>.

In the present approach there are two things to mention. In the coordinate representation and using the free, massless quark correlator<sup>7</sup>

$$S_0(-\frac{x}{2}, \frac{x}{2}) = \langle 0 | \mathcal{T} u(-\frac{x}{2}) \bar{u}(\frac{x}{2}) | 0 \rangle = -\frac{i}{2\pi^2} \frac{\not{x}}{x^4} \quad (13)$$

this second and third terms in eq. (12) would have a short-distance singularity. In the case of the vector current, one has to subtract the free propagator [29].<sup>8</sup> The disconnected parts can be shown to vanish (which follows already from current conservation [29]) and only the triangular diagram of eq. (12) survives.

For very *small* Euclidean space-time separations  $|x|, |y| \ll 0.2$  fm the 3-point function  $\Pi_\mu(x, y)$  is governed by the free Dirac propagator eq. (13). For  $x \cdot y = 0$ , which we use, it is especially simple

$$\lim_{x, y \rightarrow 0} \Pi_\mu(x, y) = -\frac{N_c e_\pi}{2\pi^6} \frac{i x_\mu}{x^4} \frac{1}{(y^2 + x^2/4)^3} \quad (14)$$

---

<sup>6</sup> In the case of effective quark or semi-bosonized quark theories like the NJL model [28] these expressions are known as the UV divergent one loop contributions, representing the polarization of the vacuum.

<sup>7</sup>Note that we are using anti-hermitian  $\gamma$ -matrices, so that eq. (13) is indeed real in Euclidean space.

<sup>8</sup> In the presence of the instanton also the non-zero modes get distorted [30,1] and some disconnected contributions still survive and are even divergent [1]. They however disappear after insertion of a path-ordered exponential  $\bar{q}(y) Q \gamma_\mu P \exp(-i \int_y^{y+\epsilon} A_\mu(z) dz_\mu) q(y+\epsilon)$  which makes the electromagnetic current gauge invariant and conserved.

For larger distances the non-perturbative effects come in. In the leading order for small distances the *vacuum dominance* approximation would suggest the following correction to eq. (13)

$$S\left(-\frac{x}{2}, \frac{x}{2}\right) = -\frac{\langle \bar{u}u \rangle}{12} \quad (15)$$

It is clear that the term of the order  $\mathcal{O}(|\bar{u}u|)$  vanishes due to spin traces, while the  $\mathcal{O}(|\bar{u}u|^2)$  contribution in this approach reads<sup>9</sup>

$$\Pi_\mu(x, y) = -\frac{N_c e_\pi}{72\pi^2} |\langle \bar{u}u \rangle|^2 i x_\mu \left( \frac{1}{(y^2 + x^2/4)^2} + \frac{1}{x^4} \right) \quad (16)$$

Compared to eq. (14), this next to leading order term has the same sign and indicates therefore an enhanced signal in this channel. This is similar to the pion two-point correlator itself [2] and can be traced back to the attractive forces inside the pion.

However such "vacuum dominance" approximation works only qualitatively and for small distances only. To go beyond those one needs a model for the non-perturbative effects. The basic feature of the instanton-based models is related to the zero mode solutions of the Euclidean Dirac operator  $\hat{D}$ , which are obtained from

$$\hat{D}\phi_\lambda = \lambda\phi_\lambda, \quad (17)$$

for  $\lambda = 0$  and exist, if the topology of the gauge field configurations is non-trivial. This is the case for the instanton solutions. From these solutions we approximate the full Dirac propagator  $S(-x/2, x/2)$  in the instanton liquid model by a sum of the zero mode contributions [1,2]  $S_{ZM}(-x/2, x/2)$ :

$$S_{ZM}\left(-\frac{x}{2}, \frac{x}{2}\right) = \sum_{I,J} \phi_I\left(-\frac{x}{2}\right) \langle I | \frac{1}{\hat{D} + m} | J \rangle \phi_J^\dagger\left(\frac{x}{2}\right) \quad (18)$$

and the non-zero mode term  $S_{NZM}(-x/2, x/2)$  [30,31]

---

<sup>9</sup>Note that it is different from the  $\mathcal{O}(\alpha_s \langle \bar{\Psi}\Psi \rangle^2)$  contribution in standard OPE analysis [9].

$$S_{NZM}(-\frac{x}{2}, \frac{x}{2}) = S_0(-\frac{x}{2}, \frac{x}{2}) + \sum_I \left[ S_I(-\frac{x}{2}, \frac{x}{2}) - S_0(-\frac{x}{2}, \frac{x}{2}) \right] \quad (19)$$

where  $S_I(-x/2, x/2)$  is the non-zero mode contribution in the presence of a single instanton<sup>10</sup>.

Before discussing the result of the full calculation with eq. (18) and eq. (19) in eq. (12) in an ensemble of instantons, it is instructive to investigate the effect of a *single* instanton, as done by Forkel and Nielsen. Then the general form of the zero mode propagator is given by

$$S_{ZM}(-\frac{x}{2}, \frac{x}{2}) = \sum_\lambda \frac{\Psi_\lambda(-\frac{x}{2})\Psi_\lambda^\dagger(\frac{x}{2})}{\lambda + im} \quad (20)$$

where  $\Psi_\lambda(x) = \sum_{I=1}^N C_I^\lambda \Psi_0^I(x - z_I)$  can be expanded in terms of the zero modes  $\Psi_0^I(x)$  of individual instantons. Now one can argue [32] that for small distances the instanton  $I_*$  closest to  $\frac{x}{2}$  and  $-\frac{x}{2}$  dominates so that the propagator can be expressed in terms of this single zero mode for an instanton/anti-instanton as

$$\begin{aligned} S_{ZM}^{\text{MF}}(-\frac{x}{2}, \frac{x}{2}) &= \sum_\lambda \frac{|C_{I_*}^\lambda|^2}{\lambda + im} \Psi_0^{I_*}(-\frac{x}{2})\Psi_0^{I_*\dagger}(\frac{x}{2}) \\ &= \frac{(-\frac{x}{2} - z)\gamma_\mu\gamma_\nu(\frac{x}{2} - z)}{8\bar{m}} \begin{pmatrix} \tau_\mu^- \tau_\mu^+ P_L \\ \tau_\mu^+ \tau_\mu^- P_R \end{pmatrix} \phi(-\frac{x}{2} - z)\phi(\frac{x}{2} - z) \end{aligned} \quad (21)$$

where a dynamically generated effective mass  $\bar{m}$  can be defined from eq. (20) by

$$\frac{1}{\bar{m}} = \sum_\lambda \frac{|C_{I_*}^\lambda|^2}{\lambda + im} \quad (22)$$

and

$$\phi(x) = \frac{\rho}{\pi |x| (x^2 + \rho^2)^{3/2}}. \quad (23)$$

---

<sup>10</sup>This expression eq. (19) should be understood as the leading term in a multiple scattering expansion, cf. [2] for details.

In this approach the effect of distant instantons and chiral symmetry breaking is therefore effectively included by replacement of the current quark mass  $m$  by  $\bar{m}$ , the dynamically generated effective mass [17], representing chiral symmetry breaking by other instantons. This was done by Forkel and Nielsen [16] who has used the correlator  $\Pi_\mu(x, y)$  with eq. (21) . In the short distance limit<sup>11</sup> this reduces to

$$\lim_{x,y \rightarrow 0} \Pi_\mu(x, y) = -\frac{ie_\pi}{5\pi^4} \frac{\bar{n}}{\bar{m}^2 \rho^4} \frac{x_\mu}{(y^2 + x^2/4)^2} \quad (24)$$

Note that using the mean field results [18,33] for the constituent quark mass<sup>12</sup> and the condensate, namely  $\langle \bar{u}u \rangle \sim \sqrt{\bar{n}}/\rho$  and  $\bar{m} \sim \sqrt{\bar{n}}\rho$ , the eq. (24) gives a correlator which is parametrically larger than eq. (16) by the inverse packing fraction  $1/f \sim 1/(\bar{n}\rho^4) \gg 1$ .

However for the full Instanton Liquid simulation the formulas of Forkel and Nielsen are consistent to our approach for short distances. But neither the vacuum dominance nor the single-instanton approach [16] can describe the correlator for larger distances  $x, y \gg 0.2$  fm necessary for a clear separation of the pion contribution. This goal will be reached in the next section, by using the numerically calculated correlators.

#### IV. CORRELATORS IN RANDOM INSTANTON VACUUM

Numerically the propagators are calculated as solutions to eqs. (18), (19). Furthermore for the RILM we took 256 randomly placed and oriented instantons (half of them anti-instantons) into a periodic box of  $(5.67)^2 \times (2.82)^2$  fm<sup>4</sup>, where the long box lengths correspond to the  $x, y$  directions, in which the correlator is actually measured. The numbers are chosen to reproduce an instanton density of  $\bar{n} = 1$  fm<sup>-4</sup>. Furthermore,

---

<sup>11</sup>See our discussion of the full expression in the next section and App.A.

<sup>12</sup>Note that it is not equal to the so called constituent quark mass (and it is in fact about twice smaller) because the effective mass in question is not evaluated at zero momentum.

we take a *variable* average instanton size ( $\rho = 0.28 \text{ fm}, 0.35 \text{ fm}, 0.42 \text{ fm}$ ) in order to show the sensitivity of the form factor to the instanton size. We have evaluated 2- and 3-point functions and studied them in detail.

In Fig.1 we show the two point correlation function. According to our pole plus resonance Ansatz (eqs. A5,A6) for the correlator we give in the figure the best fit for the pion mass  $m_\pi$  and the coupling constant  $\lambda_\pi$ . Because of our finite box we used a current quark mass of  $m_u = m_d = 20 \text{ MeV}$  which is somewhat larger than the physical quark masses. Using the Gell-Mann Oakes Renner relation, the measured pion mass values in Fig. 1 are scaled down to the physical pion mass, see Tab. (I) . The extrapolated value is close to the experimental value. For the *same configurations* we determined then these parameters by fitting the three-point correlators shown in Fig. 2. In principle the correlator is a function of two points,  $x$  and  $y$ , which we have chosen to be orthogonal. So one can separately check that the form factor has no or negligible  $x$  dependence and then look for the  $y$  dependence. The  $x$  value has to be chosen large enough, so that the correlator is clearly dominated by the pion. However if  $x$  is too large the statistical errors become too large and no extraction of the parameters of the form factor is possible. Therefore in practice we followed an alternative scheme, which covers both situations simultaneously and furthermore saves some computing time: we fixed the ratio of  $x$  and  $y$  to  $x = 2y$ . In app. B we also give formulas for the continuum contribution, though we want to stress that our parameter fixing is totally independent of this parametrization since we are considering distances  $x \gg 0.5 \text{ fm}$ , where these contributions are highly suppressed compared to the pole contribution.

The pion parameters,  $m_\pi$  and  $\lambda_\pi$ , found from 2- and 3-point correlators agree within the error bars. Established consistency, we have further determined the mass in the monopole formfactor, which actually can be done rather accurately. We have found that this mass (or the pion size) turns out to be sensitive to the instanton *size*, see

Fig.3. Remarkably enough, the experimental corridor (two horizontally dashed lines) indicate the preferred instanton size to be  $\rho = 0.35$  fm, in approximate agreement with  $1/3$  fm [18] and in very good agreement with lattice results [7] pointing out  $\rho = 0.35$  fm as well.

As can be seen in the figure a further improvement of the experimental measured formfactor, as it is planned [27], and increasing the accuracy of the instanton calculation could provide a very powerful tool actually to measure the instanton size. This is a remarkable statement since it directly connects a physical observable like the formfactor to an intrinsic property of the QCD vacuum, the size of the instantons.

In addition in Fig.7 we compared our full RILM result to the one-instanton approach of the pion formfactor of Forkel and Nielsen [16], but now plotted in coordinate space and without Borel transform. As can be seen, this approach is reliable for distances not larger than  $0.4 - 0.5$  fm. The same qualitative behaviour of the two approaches was found for the pion correlator itself [34].

## V. CORRELATORS IN INTERACTING INSTANTON VACUUM

On general grounds, the pion channel is a strongly attractive one, and it was expected that pion properties (including form factors) do not depend on the details of the instanton ensemble, such as correlations etc.

In order to check these expectations we repeated the calculations for the IILM. Our results are shown in Fig. 5 and 6 for 2- and 3-point correlators (analogous to Fig.1,2). Because of the particular interaction assumed, the ensemble has an average instanton size of  $\bar{\rho} = 0.42$  fm [19], so we are not able to compare different sizes for this model. However, by comparing the IILM with the RILM for this common size of  $\bar{\rho} = 0.42$  fm, we can find out the role of the correlations. As can be seen from Tab. (II) , we have in fact found that the pion coupling constant depends rather strongly on the model (to

a degree, this may be traced back simply to different values of the quark condensate), while the pion and the monopole mass (of the form factor) are less dependent. Within the error bars of our fits, the  $m_\pi^*$  and  $m_V$  of Tab. (II) seem to agree with the values of Tab. (I) for  $\bar{\rho} = 0.42$  fm.

The same can be done for the isovector scalar meson, the  $\delta$ , as shown in Fig. 4. However, as already mentioned, in this channel the repulsion is very large and the simple random instanton liquid does no longer give a good description of the correlator. On very general grounds, the correlator should be positive for larger distances, whereas the RILM correlator changes sign for  $x = 2y \simeq 0.6$  fm and crosses the axis again at  $x = 2y \simeq 1.4$  fm. The situation changes dramatically if we consider the IILM correlator. This one, as can be seen also in Fig. 4, stays positive over the whole range of available distances. However for  $x = 2y \simeq 1.8$  fm the error bars become larger and the correlator increases again, which is an unphysical effect. Since the mass of the  $\delta$  is too large to be measured precise enough in our model, we do not attempt to determine the mass of the possible form factor. The figure should serve only as a further qualitative justification of our IILM model, in which the correlation and interaction of the instantons provide the right behaviour for the strong repulsive channels.

The last issue we address in this work deal with the old question of *vector dominance*. We remind the reader that it suggests that a *complete* pion formfactor is given by a rho-meson pole alone, and thus the fitted mass in the formfactor  $m_V$  is nothing else but  $m_\rho$ . It is certainly approximately true in nature: and therefore we have tried to check whether indeed there exist a strong correlation between them (in the models used). Therefore we have determined also the parameters of the  $\rho$  meson correlator (shown in Fig. 8). However we found that: (i)  $m_\rho$  is only very weakly dependent on the instanton size, from 875 to 915 MeV in our given interval for the instanton sizes; (ii)  $m_\rho$  is more sensitive to correlations than  $m_V$ ; and (iii)  $m_V$  is also significantly



(more than 10%) smaller than the experimental  $m_\rho$ <sup>13</sup>. We therefore conclude, that in the instanton-based models the mass in the pion form factor  $m_V$  has nothing to do with the  $\rho$ -meson mass, and the fact that they are close numerically is probably just a coincidence.

## VI. SUMMARY AND DISCUSSION

We calculated the pion electromagnetic formfactor for space like momentum transfer, based on a three-point Euclidean correlation function of two pseudoscalar, isovector currents and an external electromagnetic current. Two variants of the instanton-based QCD vacuum models were used, a random one, RILM, and the interacting one, IILM. Our main result is the existence of the direct connection between the size of the instanton and the size of the pion.

In contrast to earlier work [16], we have calculated the correlation function in coordinate space at sufficiently large distances, clearly separating the pion pole contribution from those of non-resonance states. We have accurately determined the pion coupling constant  $\lambda_\pi$ , the pion mass  $m_\pi$  and the parameter  $m_V$  of the monopole fit to the electromagnetic formfactor. The first two parameters are fitted *both* from 2-point and 3-point correlators, and the results are consistent within errors.

We have calculated the monopole mass of the formfactor  $m_V$  for three different sets of average instanton sizes at *fixed* instanton density  $\bar{n} = 1 \text{ fm}^{-4}$  and find that it is indeed sensitive. Thus the pion size is directly related to the instanton size. Furthermore, the experimental monopole mass  $m_V \simeq 679 \pm 18 \text{ MeV}$  is only reproduced for a mean instanton size around 0.35 fm, a value consistent with direct lattice measurements [7].

---

<sup>13</sup>The latter one is in the instanton model unfortunately too large, probably due to the crudeness of our phenomenological Ansatz.

As a further check we used the streamline version [21,19] of the interacting instanton model (IILM). In this case the inverse monopole mass is small 0.16 fm, or  $m_V \simeq 1200$  MeV. It does not agree with data but agrees well with the RILM result for the same mean instanton size of  $\bar{\rho} = 0.42$  fm. These results indicate that the formfactor does not depend very much on the correlations between instantons. Other quantities like the condensates, e.g., do however depend rather strongly on which model is used and therefore on such correlations. So, the IILM can and should be improved.

We have considered the issue of vector dominance, suggesting that the formfactor mass  $m_V$  is nothing but  $m_\rho$ . However, in our model used, we have found that both quantities show different dependence on the instanton size and correlations in the ensemble. We therefore suggest that vector dominance should not hold in general and seems to be more a kind of a coincidence. This will be checked by considering other 3-point functions in forthcoming publications.

### ACKNOWLEDGMENTS

The authors acknowledge the support of Alexander von Humboldt Foundation (AB) and Department of Energy grant DE-FG02-88ER40388. Useful discussions with Th. Schaefer (INT) are acknowledged.

TABLES

	2-point		3-point			$\langle\bar{u}u\rangle^{1/3}$ [ MeV]	$m_\pi$ [ MeV]	$f_\pi$ [ MeV]
	$\lambda_\pi^{1/2}$ [ MeV]	$m_\pi^*$ [ MeV]	$\lambda_\pi^{1/2}$ [ MeV]	$m_\pi^*$ [ MeV]	$m_V$ [ MeV]			
$\rho = 0.28$	$455\pm 5$	$265\pm 5$	$455\pm 5$	$265\pm 5$	$1250\pm 50$	$280.3\pm 0.46$	139	$149.9\pm 5$
$\rho = 0.35$	$490\pm 5$	$285\pm 5$	$480\pm 5$	$290\pm 5$	$680\pm 20$	$259.1\pm 0.25$	150	$106.6\pm 5$
$\rho = 0.42$	$520\pm 5$	$255\pm 5$	$510\pm 5$	$265\pm 5$	$550\pm 20$	$245.2\pm 0.39$	136	$79.9\pm 5$

TABLE I. The pion properties in the RILM for different values of the instanton size  $\rho$ . The pion coupling constant  $\lambda_\pi$  and pion mass  $m_\pi^*$  for  $m_u = 0.1\Lambda \simeq 20$  MeV obtained from the 2-point and 3-point function are determined independently and coincide within the uncertainty of the fit. For comparison, Forkel and Nielsson used  $\lambda_\pi^{1/2} = 363$  MeV, which either corresponds to a rather low value for the condensate  $\langle\bar{u}u\rangle^{1/3} \simeq 200$  MeV or a large  $f_\pi \simeq 180$  MeV. The physical pion mass  $m_\pi$  in the table follows from an assumed Gell-Mann Oakes Renner scaling relation with  $m_u + m_d = 11$  MeV.

	2-point		3-point			$\langle\bar{u}u\rangle^{1/3}$ [ MeV]	$m_\pi$ [ MeV]	$f_\pi$ [ MeV]
	$\lambda_\pi^{1/2}$ [ MeV]	$m_\pi^*$ [ MeV]	$\lambda_\pi^{1/2}$ [ MeV]	$m_\pi^*$ [ MeV]	$m_V$ [ MeV]			
$\bar{\rho} = 0.42$	$395\pm 5$	$260\pm 5$	$370\pm 5$	$295\pm 5$	$1200\pm 50$	$217.3 \pm 0.55$	113	$93 \pm 5$

TABLE II. The pion properties in the IILM for  $\Lambda = 306$  MeV. The pion coupling constant  $\lambda_\pi$  and pion mass  $m_\pi^*$  for  $m_u = 0.1\Lambda$  obtained from the 2-point and 3-point function are determined independently. The physical pion mass  $m_\pi$  in the table follows from an assumed Gell-Mann Oakes Renner scaling relation with  $m_u + m_d = 11$  MeV.

## APPENDIX A: ONE INSTANTON FORMULAS

### 1. The pion correlator

The pion correlator for pseudoscalar currents  $j_5(x)$  for short distances in the asymptotic regime is simply given by

$$\langle 0 | T j_5(x) j_5(0) | 0 \rangle = \frac{N_c}{\pi^4} \frac{1}{x^6} := \Pi(x)_{free} \quad (\text{A1})$$

Corrections to this correlator at larger distances are given by the direct instanton contribution:

$$\begin{aligned} \langle 0 | T j_5(x) j_5(0) | 0 \rangle &= \frac{12}{\pi^2} \bar{n} \frac{1}{\bar{m}^2} \rho^4 \frac{x^2}{\sqrt{4x^2\rho^2 + x^4}} \\ &\left[ \operatorname{arctanh} \frac{x^2}{\sqrt{4x^2\rho^2 + x^4}} 8(x^4 + 2\rho^2 + 2\rho^2 x^2) + \sqrt{4x^2\rho^2 + x^4} \frac{1}{3\rho^2} (2x^4 - 10x^2\rho^2 - 12\rho^4) \right] \\ &:= \Pi(x)_{inst} \end{aligned} \quad (\text{A2})$$

where  $\bar{m}$  (cf. eq. 22) is the effective constituent quark mass [35,36] The asymptotics of the one-instanton formula eq. (A2) for short distances is given by

$$\lim_{x \rightarrow 0} \Pi(x)_{inst} = \frac{1}{\pi^2} \frac{\bar{n}}{\bar{m}^2} \rho^4 \frac{2}{5\rho^8} \quad (\text{A3})$$

which is suppressed by the free contribution eq. (A1) with the power  $x^6$ , so that the sum of  $\Pi(x)_{inst}$  and  $\Pi(x)_{free}$ , normalized with  $\Pi(x)_{free}$ , goes to unity. This is also the case for our instanton liquid ensemble of Fig.1 and 5. For large distances the limit of eq. (A2) becomes

$$\lim_{x \rightarrow \infty} \Pi(x)_{inst} = \frac{12}{\pi^2} \bar{n} \frac{1}{\bar{m}^2} \rho^4 \frac{2}{3\rho^2 x^6} \quad (\text{A4})$$

Here the zero mode contribution is proportional to the free part eq. (A1) and actually dominates the sum of both expression. For completeness the pole contribution of the 2-point function in a simple pole plus continuum Ansatz is [2] given by

$$\Pi(x)_{pole} = \frac{\lambda_\pi^2}{4\pi^2} \frac{1}{x^2} m_\pi |x| K_1(m_\pi |x|) \quad (\text{A5})$$

whereas the continuum results [2] reads

$$\Pi(x)_{cont} = \frac{3}{16\pi^6} \left( K_1(Ex)(16Ex + 4(Ex)^3) + K_0(Ex)(8(Ex)^2 + (Ex)^4) \right) \quad (\text{A6})$$

Indeed the small size limit of eq. (A6) for a fixed threshold  $E$  is given by

$$\lim_{Ex \rightarrow 0} \Pi(x)_{cont} = \Pi(x)_{free} \quad (\text{A7})$$

whereas the normalized pole contribution, i.e.  $\lim_{x \rightarrow 0} \Pi(x)_{pole}/\Pi(x)_{free}$ , vanishes.

## 2. The pion EM-formfactor

From our general expression eq. (12) and the one-instanton Ansatz eq. (21) the correlator is given by

$$\begin{aligned} \Pi_\mu(x, y) = & \frac{-ie_\pi}{\pi^6} \frac{4\bar{n}\rho^4}{\bar{m}^2} \frac{1}{(y^2 + x^2/4)^2} \int d^4z \\ & \frac{y_\mu(x^2/4 + 2yz - z^2) + x_\mu/2(-y^2 + 2yz - z^2) + z_\mu(-y^2 - x^2/4)}{|y-z|((y-z)^2 + \rho^2)^{1.5}((x/2-z)^2 + \rho^2)^3 |x/2+z|((x/2+z)^2 + \rho^2)^{1.5}} \end{aligned} \quad (\text{A8})$$

where the trivial averaging over color orientations is already done. The averaging over the instanton position in eq. (A8) can be performed after introducing 5 Feynman parameter integrals for the 5 denominators in eq. (A8). After this, it is even possible to perform 2 of the Feynman integrals analytically, which results in the rather awkward expression

$$\begin{aligned} \Pi_\mu(x, y) = & \frac{e_\pi}{\pi^8} \frac{\bar{n}\rho^4}{\bar{m}^2} 5760 \frac{-ix_\mu}{(y^2 + x^2/4)^2} \int_0^1 da_1 \int_0^{1-a_1} da_2 \int_0^{1-a_1-a_2} da_3 a_1^2 \sqrt{\frac{a_2}{a_3}} \\ & \left[ \frac{\pi^3(1-a_1-a_2)}{3840} \frac{35b^3 + 120ab^2 + 144ba^2 + 64a^3}{a^{4.5}(a+b)^{3.5}} \right. \\ & \left. \left( x^2/4((a_1-a_2-a_3)^2 + (a_1-a_2-a_3)) + y^2((a_1+a_2+a_3)^2 + (a_1-a_2-a_3)) \right) \right. \\ & \left. + \frac{\pi^3(1-a_1-a_2)}{960} \frac{5b^2 + 12ba + 8a^2}{a^{3.5}(a+b)^{2.5}} \right] \end{aligned} \quad (\text{A9})$$

where

$$a = \rho^2(1 - a_3) + x^2/4((a_1 + a_2 + a_3) - (a_1 - a_2 - a_3)^2) + y^2((a_1 + a_2 + a_3) - (a_1 + a_2 + a_3)^2) \quad (\text{A10})$$

and  $b = -\rho^2(1 - a_1 - a_2 - a_3)$ . Similiar to the 2-point function one can consider the short distance behaviour of this function and finds

$$\lim_{x,y \rightarrow 0} \Gamma_\mu(x, y, 0) = -\frac{e_\pi}{5\pi^4} \frac{\bar{n}}{m^2 \rho^4} \frac{ix_\mu}{(y^2 + x^2/4)^2} \quad (\text{A11})$$

Because our triangular diagram for the EM form factor in this approximation actually consists of 2 zero mode propagators and one free propagator, the zero mode part reduces to a constant, similiar to eq. (A3) , and a single quark propagator in eq. (A11) remains. The full behaviour of eq. (A9) can be seen in Fig. 7 compared to the full (RILM) result. Obviously the one instanton formula deviates from the full result for distances larger than 0.4 fm.

## APPENDIX B: CONTINUUM CONTRIBUTION

For the continuum contribution one has to calculate the double discontinuity of the spectral density from the expression for the triangular diagram according to the Cutkovsky rule as

$$\rho_\mu(s_1, s_2, Q^2) = \frac{N_c}{\pi^2} \frac{1}{4\pi} \int \frac{d^4 k}{(2\pi)^4} \theta(k_0) \delta(k^2) \theta(k_0 - p_0) \delta((k - p)^2) \theta(k_0 - p'_0) \delta((k - p')^2) \quad (\text{B1})$$

with the result [9]

$$\rho_\mu(s_1, s_2, -q^2) = \frac{s_1 s_2}{\pi^2} \frac{N_c}{\lambda^{1.5}} \left[ \bar{p}_\mu q^2 - q_\mu (s_2 - s_1) / 4 \right] \quad (\text{B2})$$

where  $\lambda = (s_1 + s_2 + q^2)^2 - 4s_1 s_2$ . Inserting this into the dispersion relation and transforming the resulting expression into Euclidean space, one can use the Feynman

parameters as before for the pole contribution to perform the  $\bar{p}$ -integration analytically. In order to model the continuum one usually introduces a threshold parameter  $s_0$  into dispersion relations. If one does it, the continuum contribution reduces to a four dimensional integral, which can be easily done numerically. It reads

$$\begin{aligned} \Pi_{\mu,cont}(x, y) = & -iN_c \int_0^\infty ds_1 ds_2 \int_0^1 d\alpha \int_0^\infty dq (1 - \theta(s_1 - s_0)\theta(s_2 - s_0)) \frac{N_c}{64\pi^6} \frac{s_1 s_2 q^2}{\lambda^{1.5}} \\ & \left[ q^2 M \frac{x_\mu}{|x|} K_1(|x| M) \frac{J_1(q |y + x(0.5 - \alpha)|)}{|y + x(0.5 - \alpha)|} \right. \\ & \left. \frac{(s' - s)}{4} K_0(|x| M) \frac{1}{|y + x(0.5 - \alpha)|^2} (J_0(q |y + x(0.5 - \alpha)|) q (y_\mu + x_\mu(0.5 - \alpha))) \right. \\ & \left. - 2J_1(q |y + x(0.5 - \alpha)|) \frac{y_\mu + x_\mu(0.5 - \alpha)}{|y + x(0.5 - \alpha)|} \right] \end{aligned} \quad (\text{B3})$$

where

$$M^2 = q^2 \alpha(1 - \alpha) + s\alpha + (1 - \alpha)s' > 0 \quad (\text{B4})$$

and  $\lambda = (s_1 + s_2 + q^2)^2 - 4s_1 s_2$ . In eq. (B3) we introduced a simple model for the continuum by introducing the  $\theta$ -functions [24]. Below we argue why their detailed form is not important here.

Now considering our preferred geometrical arrangement  $x \cdot y = 0$  it is clear from eq. (B3) that the  $x_\mu$  part in the last two lines vanishes due to the  $\alpha$ -integration. Finally the  $y_\mu$  terms vanishes because these are antisymmetric in  $s \leftrightarrow s'$ <sup>14</sup>. Therefore only the first term in eq. (B3) finally contributes, so that

$$\begin{aligned} \Pi_{\mu,pole}(x, y) + \Pi_{\mu,cont}(x, y) = & \\ & -i \int_0^\infty dq \int_0^1 d\alpha \frac{q^2}{32\pi^4} \left[ \frac{J_1(q |y - x(0.5 - \alpha)|)}{|y - x(0.5 - \alpha)|} \sqrt{m_\pi^2 + q^2 \alpha(1 - \alpha)} \right. \\ & \left. K_1 \left( |x| \sqrt{m_\pi^2 + q^2 \alpha(1 - \alpha)} \right) \frac{2\lambda_\pi^2 e_\pi}{1 + q^2/m_V^2} \frac{x_\mu}{|x|} \right] \end{aligned}$$

---

<sup>14</sup>Using that  $M^2$  is invariant under simultaneous change of  $s \leftrightarrow s'$  and  $\alpha \leftrightarrow (1 - \alpha)$  as well as the remainder of the formula eq. (B3) .

$$\begin{aligned}
& + \int_0^\infty ds_1 \int_0^\infty ds_2 (1 - \theta(s_1 - s_0)\theta(s_2 - s_0)) \frac{N_c}{2\pi^2} \frac{s_1 s_2 q^2}{\lambda^{1.5}} \frac{x_\mu M}{|x|} \\
& K_1(|x|M) \frac{J_1(q|y+x(0.5-\alpha)|)}{|y-x(0.5-\alpha)|} \Big] \tag{B5}
\end{aligned}$$

Similar to the 2-point function eq. (A6) the small size limit of eq. (B5), which is actually the small size limit of  $\Pi_{\mu,cont}(x, y)$ , is given by  $\Pi_\mu(x, y)$  of eq. (14). First one should note that eq. (B5) is finite with neither referring to subtraction terms, which would be necessary in momentum space due to the insufficient fast decreasing spectral density, nor to Borel transformations. The latter method eliminates the subtraction terms, because these are known to be polynomials in either  $p$  or  $p'$  and therefore vanish after taking derivatives finite times [24]. In the present approach, the Fourier transform of the dispersion relation into coordinate space, which is finite a priori, circumvents the introduction of any subtractions. However one should also stress, that the continuum contribution for a threshold of  $s_0 > 1$  GeV is highly suppressed for distances above 1 fm. We have given those expressions for completeness and their inclusion does not affect our parameter fixing at all.



## REFERENCES

- [1] E. Shuryak and J. Verbaarschot, Nucl. Phys. **B410**, 37 (1993).
- [2] E. Shuryak and J. Verbaarschot, Nucl. Phys. **B410**, 55 (1993).
- [3] T. Schäfer, E. V. Shuryak, and J. J. M. Verbaarschot, Nucl. Phys. **B412**, 143 (1994).
- [4] D. D. Diakonov, Chiral Symmetry Breaking by Instantons, Lectures given at the Enrico Fermi School in Varenna, June 27-July 7, 1995, 1995.
- [5] E. Shuryak, Rev. Mod. Phys. **65**, 1 (1993).
- [6] M. Chu, J. Grandy, S. Huang, and J. Negele, Phys. Rev. **D49**, 6039 (1994).
- [7] M. C. Chu, J. M. Grandy, S. Huang, and J. W. Negele, Phys. Rev. **D49**, 6039 (1994).
- [8] C. Michael and P. S. Spencer, Phys. Rev. **D52**, 4691 (1995).
- [9] B. Ioffe and A. Smilga, Phys. Lett. **B114**, 353 (1982).
- [10] A. Radyushkin, Act. Phys. Polon. **26**, 2067 (1995).
- [11] G. Lepage and S. Brodsky, Phys. Rev. **D22**, 2157 (1980).
- [12] C. Roberts, Electromagnetic Pion Form Factor and Neutral Pion Decay Width, Argonne report No. ANL-PHY-7842-94, 1994.
- [13] K. Liu *et al.*, Phys. Rev. **D49**, 4755 (1994).
- [14] W. Andersen and W. Wilcox, Current Overlap Analysis of Pi and Rho Mesons, BU/HEPP/95-02, 1995.
- [15] S. Dong and J.-F. Laga, Phys. Rev. **D49**, 4755 (1994).

- [16] H. Forkel and M. Nielsen, Phys. Lett. **B345**, 55 (1995).
- [17] E. V. Shuryak, Nucl. Phys. **B214**, 237 (1983).
- [18] E. Shuryak, Nucl. Phys. **B203**, 93 (1982).
- [19] T. Schaefer and E. Shuryak, Hadronic Correlation Functions in the Interacting Instanton Liquid, SUNY-NTG-23-95, 1995.
- [20] T. Schaefer and E. Shuryak, The interacting Instanton Liquid in QCD at zero and finite Temperature, SUNY-NTG-22-95, 1995.
- [21] E. Shuryak and J. Verbaarschot, Phys. Rev. **D52**, 295 (1995).
- [22] B. Ioffe and A. Smilga, Nucl. Phys. **B216**, 373 (1983).
- [23] B. Ioffe, Phys. At. Nucl. **58**, 1408 (1995).
- [24] B. Ioffe and A. Smilga, Nucl. Phys. **B216**, 373 (1983).
- [25] C. Bebek *et al.*, Phys. Rev. **D17**, 1693 (1978).
- [26] S. Amendolia *et al.*, Nucl. Phys. **B277**, 168 (1986).
- [27] D. Mack, The Charged Pion Form Factor, proposal CEBAF Experiment 93-021, 1993.
- [28] C. Christov *et al.*, Baryons as non-topological chiral solitons, Prog. Part. Nucl. Phys. **37**(1996) to appear, 1996.
- [29] B.V.Geshkenbein and B.L.Ioffe, Nucl. Phys. **B166**, 340 (1980).
- [30] L. S. Brown, R. D. Carlitz, D. B. Creamer, and C. Lee, Phys.Rev. **D17**, 1583 (1978).
- [31] A.M.Din, J. Finjord, and W. Zakrzewski, Nucl. Phys. **B153**, 46 (1979).

- [32] T. Schaefer, E. Shuryak, and J. Verbaarschot, Instantons in QCD and related theories, in preparation, 1996.
- [33] D. Diakonov and V. Petrov, Sov. Phys. JETP **62**, 204 (1985).
- [34] T. Schaefer, private communication.
- [35] M. Shifman, A. Vainshtein, and V. Zakharov, Nucl.Phys. **B165**, 45 (1980).
- [36] C. G. Callan, R. Dashen, and D. J. Gross, Phys. Rev. **D17**, 2717 (1978).

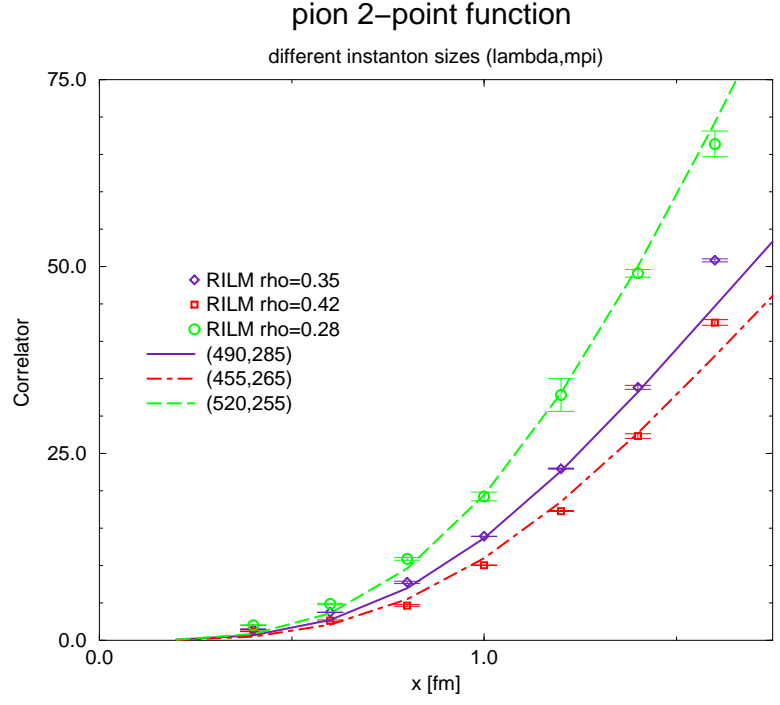


Fig. 1: The two-point correlation function of the pion, normalized to the free correlator and for three different instanton sizes in the random configuration (RILM). The instanton density is kept constant  $\bar{n} = 1 \text{ fm}^{-4}$ . The parameters of the pole contribution,  $\lambda_\pi$  and  $m_\pi$ , are given in the legend.

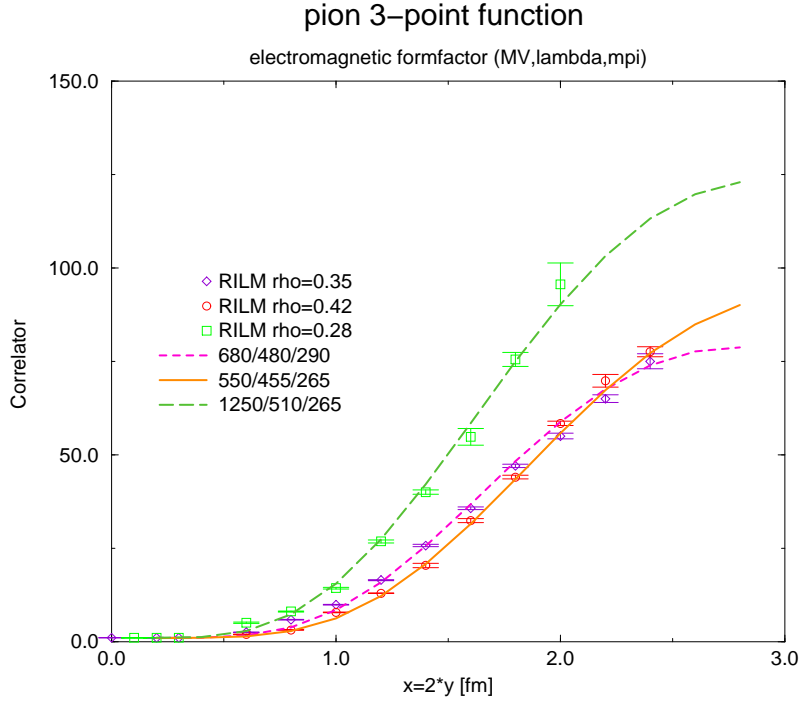


Fig. 2: The three-point correlation function of the pion and an external electromagnetic current, normalized to the free correlator and for three different instanton sizes in the random configuration (RILM). The instanton density is kept constant  $\bar{n} = 1 \text{ fm}^{-4}$ . The parameters of the pole contribution,  $m_V$ ,  $\lambda_\pi$  and  $m_\pi$  in this order, are given in the legend.

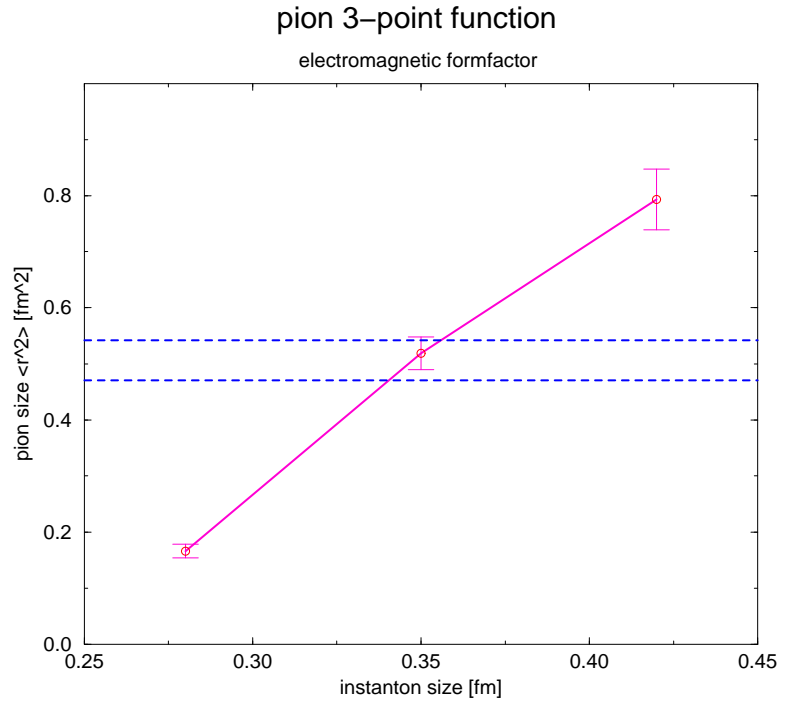


Fig. 3: The squared electromagnetic radius of the pion as a function of instanton size for the random ensemble (RILM). The instanton density is kept constant  $\bar{n} = 1 \text{ fm}^{-4}$ .

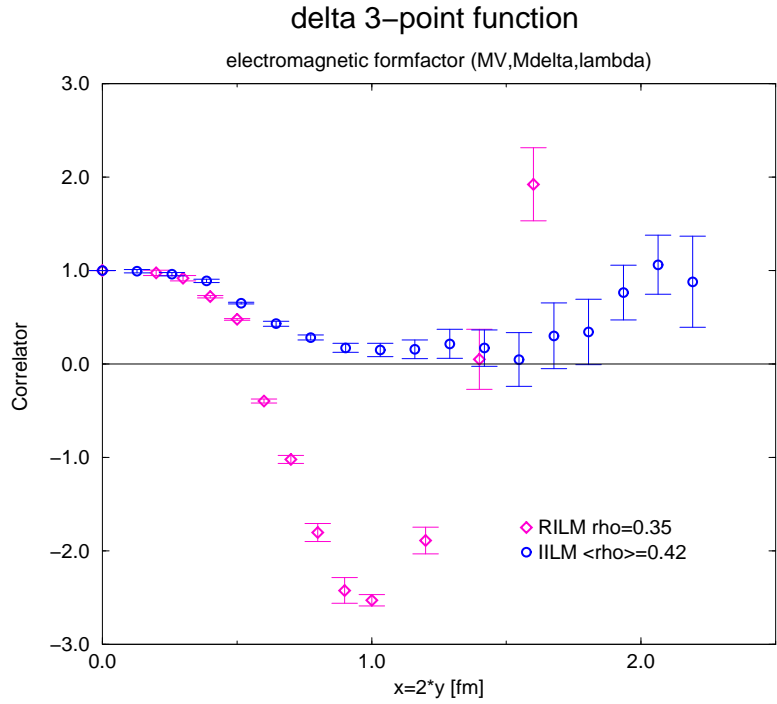


Fig. 4: The three-point correlation function of the delta (scalar, isovector) and an external electromagnetic current, normalized to the free correlator in the random configuration (RILM) and the interacting ensemble (IILM). The instanton density is kept constant  $\bar{n} = 1 \text{ fm}^{-4}$ .

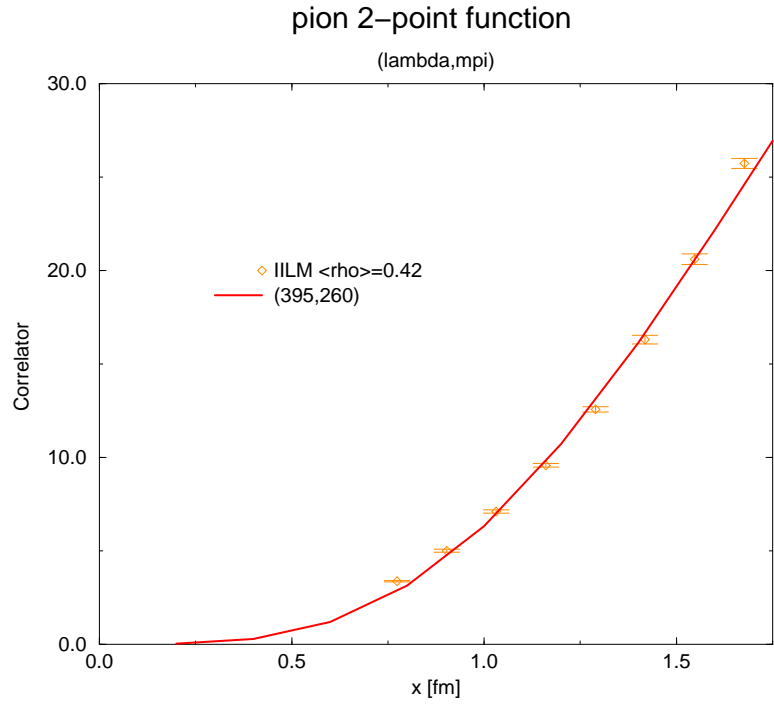


Fig. 5: The two-point correlation function of the pion, normalized to the free correlator and in the interacting configuration (IILM). The average instanton size is  $\bar{\rho} = 0.42$  fm and instanton density is  $\rho = 1 \text{ fm}^{-4}$ .



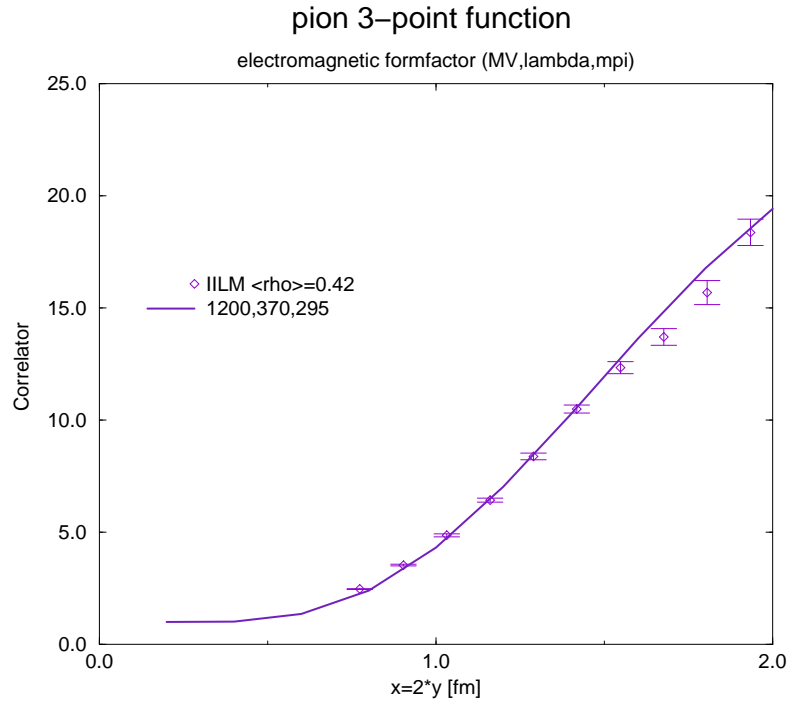


Fig. 6: The three-point correlation function of the pion and an external electromagnetic current, normalized to the free correlator and for the interacting configuration (IILM). The averaged instanton size is  $\bar{\rho} = 0.42$  fm and the instanton density is  $\rho = 1$  fm<sup>-4</sup>.

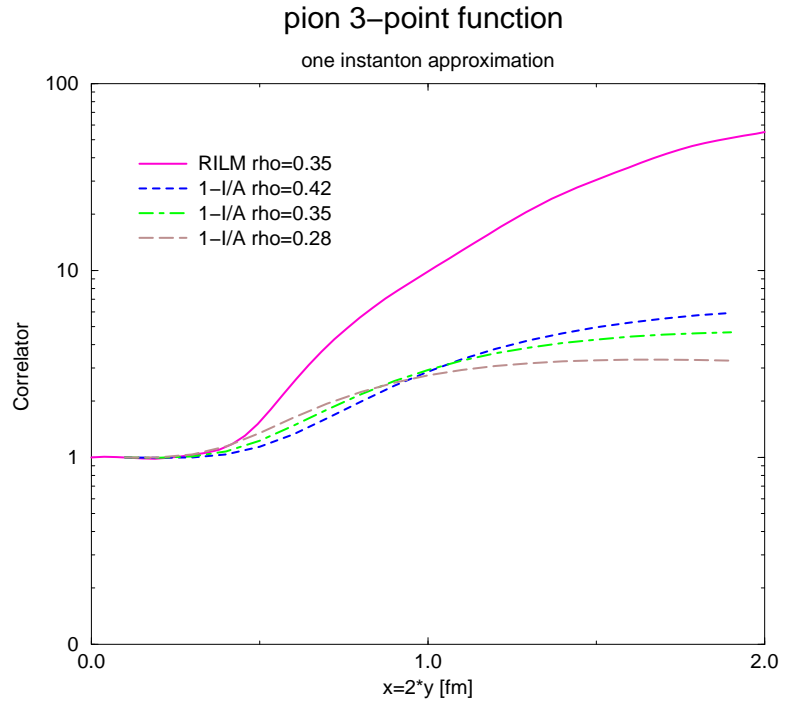


Fig. 7: The three-point correlation function of the pion and an external electromagnetic current for the RILM and the one-instanton (1inst) formula for three different instanton sizes.

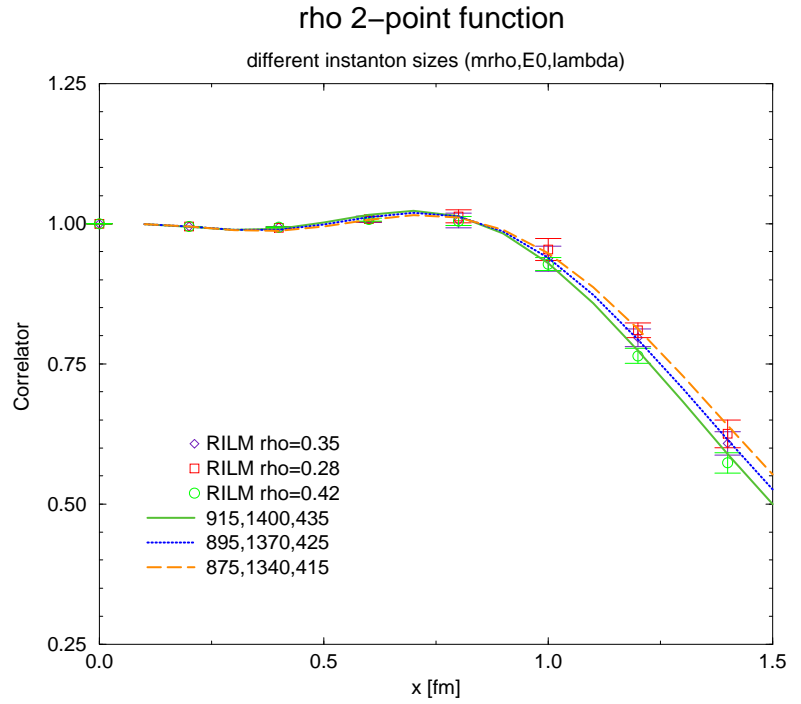


Fig. 8: The two-point correlation function of the  $\rho$ -meson for the RILM and three different instanton sizes, normalized to the two-point correlation function. In the legend, the  $\rho$  meson mass, the threshold parameter  $E_0$  and the  $\rho$  coupling constant are given.

# pion 3-point function

electromagnetic formfactor

